PERGAMON

Polyhedron 18 (1999) 755–762

POLYHEDRON

Complexes of copper(II) acetate with nicotinamide: preparation, characterization and fungicidal activity; crystal structures of $[Cu_2(O_2CCH_3)_4(nia)]$ and $[Cu_2(O_2CCH_3)_4(nia)_2]$

Bojan Kozlevčar[a,*], Ivan Leban[a], Iztok Turel[a], Primož Šegedin[a], Marko Petrič[b], Franc Pohleven[b], Andrew J. P. White[c], David J. Williams[c], Joachim Sieler[d]

[a]*Faculty of Chemistry and Chemical Technology, University of Ljubljana, Aškerčeva 5, P.O. Box 537, 1001 Ljubljana, Slovenia*
[b]*Department of Wood Science and Technology, Biotechnical Faculty, University of Ljubljana, Rožna dolina, C. VIII/34, 1000 Ljubljana, Slovenia*
[c]*Department of Chemistry, Imperial College of Science, Technology and Medicine, South Kensington, London SW7 2AY, U.K.*
[d]*Institut für Anorganische Chemie, Universität Leipzig, Linnestraße 3, 04103 Leipzig, Germany*

Received 23 July 1998; accepted 29 September 1998

Abstract

Three new copper(II) acetate complexes with nicotinamide (nia) were synthesized, analyzed and characterized by standard chemical and physical methods and tested for fungicidal activity. The crystal and molecular structures of the compounds $[Cu_2(O_2CCH_3)_4(nia)]$ (**1B**) and $[Cu_2(O_2CCH_3)_4(nia)_2]$ (**2**) were determined by X-ray diffraction. Both consist of binuclear units of bridging tetracarboxylate type, however they differ in the bonding mode of nicotinamide molecules. They are bonded at the apical positions of the dimers and connect them in an infinite chain in **1B**. On the other hand the dimers remain isolated in the structure of the compound **2**. It seems that compound **1B** is the first example where a nicotinamide molecule acts as a bidentate bridging ligand. The results of EPR spectra agree with the dimeric nature of the complexes. Dissolved in water or DMSO, the compounds completely stop mycelial growth at a concentration of 5.0×10^{-3} mol l^{-1}. Less concentrated solutions (up to 1.0×10^{-3} mol l^{-1}) show weaker fungicidal activity.

Keywords: Copper(II) acetates; Crystal structure; EPR; Bridging nicotinamide; Polymer; Fungicidal activity

1. Introduction

The preparation, structure and properties of several copper(II) carboxylates have already been extensively studied, especially with nitrogen donor ligands [1–4]. The results of some experiments show the increased activity of metal ions with the addition of some already biologically active substances. Many of such complexes are used as pharmaceuticals [5]. Our interest in the coordination chemistry of copper(II) carboxylate complexes arises in part from the fact that these type of compounds can be used as wood preservatives [6–8]. Coordination compounds with nicotinamide are potentially interesting because copper(II) carboxylates as well as nicotinamide influence biological systems. It was noticed, that the coordination of the ligands around a metal ion is important in the complex fungicidal activity. Especially interesting are binuclear copper carboxylates. The synthesis and characterization of the coordination compounds in the same system with different bonding modes of the constituents and examination of their fungicidal activity was therefore the aim of our work.

2. Experimental

2.1. Preparation of the complexes

Starting substances ($[Cu_2(O_2CCH_3)_4(H_2O)_2]$ and nicotinamide) are commercially available and were used without further purification.

2.1.1. $[Cu_2(O_2CCH_3)_4(nia)]$-A (**1A**)

Methanol (30 cm^3) was acidified with a few drops of acetic acid and finely ground copper(II) acetate hydrate (0.40 g) was added. It was dissolved by heating to boiling point and then added to 0.20 g of nicotinamide dissolved in 5 cm^3 of methanol. Soon, bright green aggregated crystals were observed. They were filtered off the following day and dried for a few hours in a desiccator over KOH.

* Corresponding author.

0277-5387/99/$ - see front matter
PII: S0277-5387(98)00350-7

Average yield of the product was 70%. *d*-Spacings (Å) (relative intensities are in parentheses): 10.5 (2), 7.49 (3), 7.40 (1), 7.15 (2), 6.70 (10), 6.50 (1), 6.38 (1), 6.27 (8), 5.41 (1), 5.26 (4). Magnetic susceptibility: μ_{eff}, 1.44 BM. IR: $\nu_{asym}(CO_2)$, 1616 cm^{-1}, $\nu_{sym}(CO_2)$, 1430 cm^{-1}. UV–Vis: 306, 375, 716 nm.

2.1.2. *[Cu$_2$(O$_2$CCH$_3$)$_4$(nia)]-B (**1B**)*

The second modification of the compound was prepared by a slightly different procedure. The solutions of the starting substances were twice more concentrated as described for **1A** and a blue–green product was filtered off after 7 days. The average yield of the product was 90%. *d*-Spacings (Å) (relative intensities are in parentheses): 11.0 (1), 10.2 (1), 7.51 (10), 7.42 (2), 7.10 (8), 6.51 (3), 6.38 (7), 6.23 (6), 5.46 (4), 5.11 (1). The observed values are in agreement with those calculated [9] from unit cell dimensions. Magnetic susceptibility: μ_{eff}, 1.47 BM. IR: $\nu_{asym}(CO_2)$, 1620 cm^{-1}, $\nu_{sym}(CO_2)$, 1435 cm^{-1}. UV–Vis: 307, 374, 727 nm.

2.1.3. *[Cu$_2$(O$_2$CCH$_3$)$_4$(nia)$_2$] (**2**)*

With the exception of a higher amount of nicotinamide (1.60 g), this compound was prepared by the same procedure as for compound **1A**. Turquoise aggregated crystals were filtered off after 2 days. The average yield was 80%. *d*-Spacings (Å) (relative intensities are in parentheses): 9.4 (2), 8.6 (10), 8.2 (5), 6.36 (5), 6.07 (3), 5.40 (2), 5.28 (1), 4.99 (2), 4.70 (1), 4.43 (1). The observed values are in agreement with those calculated [9] from unit cell dimensions. Magnetic susceptibility: μ_{eff}, 1.48 BM. IR: $\nu_{asym}(CO_2)$, 1610 cm^{-1}, $\nu_{sym}(CO_2)$, 1422 cm^{-1}. UV–Vis: 298, 373, 712 nm.

2.1.4. *[Cu$_2$(O$_2$CCH$_3$)$_4$(nia)$_2$·2H$_2$O] (**3**)*

A different procedure as already described [10] was used for the preparation of this substance. Finely ground copper(II) acetate hydrate (1.60 g) was dissolved in 25 cm^3 of acidified water. The obtained solution was added to 0.98 g of nicotinamide dissolved in 6 cm^3 of water. The solution was left to stand for 2 days at room temperature. Dark green aggregated crystals were dried for 1 day in a desiccator over KOH. The average yield of the product was 65%. *d*-Spacings (Å) (relative intensities are in parentheses): 10.1 (2), 8.0 (8), 7.32 (10), 6.43 (3), 6.21 (4), 5.74 (1), 5.65 (2), 5.12 (6), 4.36 (1), 3.69 (1). The observed values are in agreement with those calculated [9] from unit cell dimensions [11]. Magnetic susceptibility: μ_{eff}, 1.47 BM. IR: $\nu_{asym}(CO_2)$, 1616 cm^{-1}, $\nu_{sym}(CO_2)$, 1448, 1424 cm^{-1}. UV–Vis: 277, 375 (sh), 716 nm.

2.2. Physical measurements

Interplanar spacings and relative intensities were obtained by the Guinier-de-Wolf camera (Enraf Nonius) and Cu-K_α radiation. Vibrational spectra were measured in the region between 4000 and 220 cm^{-1} with a Perkin-Elmer FT-IR 1720X spectrophotometer using Nujol and poly(chlorotrifluoroethylene) oil suspension techniques. Electronic spectra were recorded as Nujol mulls (200–860 nm) with a Perkin-Elmer UV/VIS/NIR Spectrometer Lambda 19. Room temperature magnetic susceptibility measurements of powdered samples were performed by a Sherwood Scientific MBS-1 balance using $Hg[Co(NCS)_4]$ as a calibrant. Diamagnetic corrections were applied using Pascal's constants and the effective magnetic moments were calculated from the expression: $\mu_{eff} = 2.828(\chi_M T)^{1/2}$. Thermograms were recorded by the instrument Mettler TA 2000 in an argon atmosphere (flux, 35 ml min^{-1}) in the temperature range 15–500°C at a heating rate of 2 K min^{-1}. The crucible material was Pt with reference substance α-Al_2O_3. Approximately 20 mg of the sample was used. The EPR spectra of the powdered samples were recorded by a Bruker ESP-300 spectrometer, operating at the X-band at room temperature and at 150 K. The values of parameters $g_\parallel$, $g_\perp$, D and J were calculated directly with the field positions $H_\perp$, H_{z1} and H_{z2} from the spectra as described in the literature (Refs. [12, 13] and references therein).

2.3. Elemental analysis

The elemental analysis of compounds **1A**, **1B**, **2** and **3** is shown in Table 1.

Table 1
Elemental analysis

	Cu (%)		C (%)		H (%)		N (%)	
Compound	Found	Calculated	Found	Calculated	Found	Calculated	Found	Calculated
1A	26.0	26.2	34.6	34.6	3.65	3.75	6.03	5.77
1B	26.1	26.2	34.4	34.6	3.62	3.75	5.99	5.77
2	20.7	20.9	39.3	39.5	3.77	3.99	9.40	9.22
3	19.3	19.8	37.1	37.3	4.16	4.38	8.76	8.71

Anal. calc. for H_2O (**3**): 5.6%. Found: 5.2%. The presence of water in the compounds **1A**, **1B** and **2** was not observed (thermogravimetrical analysis).

2.4. X-ray crystallography of katena-(μ-nicotinamido-O,N-py)-tetrakis(μ-acetato-O,O′)dicopper(II), (1B) and tetrakis(μ-acetato-O,O′)-bis(nicotinamide)dicopper(II) (2)

Data were collected on CAD-4 diffractometer with Mo-K_α radiation for **1B** and on a Siemens P4/PC diffractometer with Cu-K_α radiation for **2**, using graphite monochromator in both cases. The data were corrected for Lorentz and polarization factors. Both structures were solved by direct methods and all non-hydrogen atoms were refined anisotropically. The amino hydrogen atoms were located from a ΔF map and refined isotropically in **1B**, but the distance constraint of 0.90 Å for N–H was applied for **2**. The positions of the remaining hydrogen atoms were idealized, assigned isotropic thermal parameters, $U(H) = 1.2U_{eq}(C)$ [$U(H) = 1.5U_{eq}$(C–Me)] and allowed to ride on their parent atoms. Refinements were by full-matrix least-squares based on F^2. Computations were carried out using the SHELXL93 and SHELXTL PC [14, 15] program systems for **1B** and **2**, respectively. The crystallographic data are summarized in Table 2. Selected bond lengths and angles are presented in Table 3. Additional material available from the Cambridge Crystallographic Data Center comprises atomic coordinates, bond lengths, angles and thermal parameters.

2.5. Screening of the compounds for fungicidal activity

The studied compounds were tested for fungicidal activity of wood-decay fungus *Trametes versicolor* (L. ex Fr.) Pilat. The same procedure was applied as described earlier [16].

3. Results and discussion

Compounds $[Cu_2(O_2CCH_3)_4(nia)]$-A (**1A**), $[Cu_2(O_2CCH_3)_4(nia)]$-B (**1B**), $[Cu_2(O_2CCH_3)_4(nia)_2]$ (**2**) and $[Cu_2(O_2CCH_3)_4(nia)_2{\cdot}2H_2O]$ (**3**), (nia, nicotinamide) were synthesized and characterized by several methods. The crystal structure and EPR spectra of the compound **3** have already been described (Refs. [11, 17] and references therein). We managed to get single crystals for **1B** and **2** but not for compound **1A** that has the same stoichiometry as **1B**. The results of other methods are comparable for both substances but powder diffraction technique proves that the compounds are not equal.

Table 2
The crystal data, data collection and structure refinement parameters for **1B** and **2**

Compound	**1B**	**2**
Formula	$C_{14}H_{18}N_2O_9Cu_2$	$C_{20}H_{24}N_4O_{10}Cu_2$
Crystal colour	blue–green	turquoise
Crystal dimensions (mm)	$0.22 \times 0.20 \times 0.40$	$0.33 \times 0.17 \times 0.17$
System	triclinic	triclinic
Space group	P-1 (No. 2)	P-1 (No. 2)
a (Å)	8.383(1)	7.203(1)
b (Å)	10.234(1)	9.530(1)
c (Å)	11.098(1)	10.732(1)
α (°)	90.69(1)	65.89(1)
β (°)	98.36(1)	73.48(1)
γ (°)	91.60(1)	81.86(1)
V (Å^3)	941.5(2)	644.4(1)
Z	2	1
λ (Å)	0.71073	1.54178
Scan mode	$\omega/2\theta$	ω
θ range for data collection (°)	1.85 to 26.1	4.66 to 59.96
h, k, l ranges	−9 8, −12 12, −9 13	−8 7, −9 9, −11 12
Data measured	4365	2014
Unique data	3184	1843
Observed data $\lvert F_0\rvert > 4\sigma(\lvert F_0\rvert)$	2916	1659
Variables	253	172
Data/restraints/parameters	3184/0/253	1835/2/172
Goodness-of-fit on F^2	1.044	1.078
Final R indices $\lvert F_0\rvert > 4\sigma(\lvert F_0\rvert)$	$R_1 = 0.0311$, $wR_2 = 0.0810$	$R_1 = 0.0404$, $wR_2 = 0.1016$
R indices (all data)	$R_1 = 0.0352$, $wR_2 = 0.0844$	$R_1 = 0.0476$, $wR_2 = 0.1102$
Extinction coefficient	0.0036(8)	0.0050(12)
Maximum, minimum residue (e Å^{-3})	0.329, −0.573	0.439, −0.421
Mean, maximum shift/error	0.005, 0.111	0.000, −0.001

Table 3
Selected bond lengths (Å) and angles (°) with estimated standard deviations in parentheses

	1B[a]	**2**[a]		**1B**[b]
Bonds (Å)				
Cu(1)–O(12A)	1.968(2)	1.959(3)	Cu(2)–O(32B)	1.967(2)
Cu(1)–O(11)	1.968(2)	1.958(3)	Cu(2)–O(31)	1.968(2)
Cu(1)–O(22A)	1.979(2)	1.971(3)	Cu(2)–O(42B)	1.973(2)
Cu(1)–O(21)	1.989(2)	1.993(3)	Cu(2)–O(41)	1.999(2)
Cu(1)–N(1)	2.158(2)	2.172(3)	Cu(2)–O(1)	2.146(2)
Angles (°)				
O(12A)–Cu(1)–N(1)	95.48(9)	95.69(11)	O(32B)–Cu(2)–O(1)	96.46(9)
O(11)–Cu(1)–N(1)	96.15(9)	95.88(11)	O(31)–Cu(2)–O(1)	95.04(9)
O(22A)–Cu(1)–N(1)	94.21(9)	94.26(11)	O(42B)–Cu(2)–O(1)	98.02(8)
O(21)–Cu(1)–N(1)	97.54(9)	97.17(11)	O(41)–Cu(2)–O(1)	93.47(8)
O(12A)–Cu(1)–O(11)	168.37(9)	168.38(11)	O(32B)–Cu(2)–O(31)	168.49(9)
O(12A)–Cu(1)–O(22A)	89.68(11)	91.47(12)	O(32B)–Cu(2)–O(42B)	89.72(11)
O(11)–Cu(1)–O(22A)	89.58(11)	88.72(12)	O(31)–Cu(2)–O(42B)	88.50(10)
O(12A)–Cu(1)–O(21)	89.05(10)	87.72(12)	O(32B)–Cu(2)–O(41)	88.02(10)
O(11)–Cu(1)–O(21)	89.31(11)	89.80(11)	O(31)–Cu(2)–O(41)	91.47(9)
O(22A)–Cu(1)–O(21)	168.25(9)	168.57(10)	O(42B)–Cu(2)–O(41)	168.47(9)

[a]Coordination sphere around the Cu(1) for **1B** and **2**.
[b]Coordination sphere around the Cu(2) for **1B**.

*3.1. Crystal and molecular structures of $[Cu_2(O_2CCH_3)_4(nia)]$-B (**1B**) and $[Cu_2(O_2CCH_3)_4(nia)]$ (**2**)*

The X-ray analysis of the $[Cu_2(O_2CCH_3)_4(nia)]$ **1B** revealed a polymeric structure composed of two tetracarboxylates, each positioned about an independent centre of symmetry (Fig. 1). Every second dimer is bonded with two nicotinamide molecules as in related compound **2** with isolated tetracarboxylates (Fig. 2). In these two structures the planes of the pyridine ring are inclined by 9 (13°) and 84 (81°) for **1B** (**2**) to the Cu/O(11)/C(11)/O(12)/CuA and Cu/O(21)/C(21)/O(22)/CuA coordination planes, respectively. Interestingly the Cu–O acetate bonds that lie close to the plane of the pyridine ring are consistently shorter than those that are directed orthogonally, a pattern that is observed in both structures Table 3. The principal difference between both complexes is observed at nicotinamide molecules that are in a polymeric compound not bonded only with pyridine nitrogen but also with amido oxygen to an adjacent copper center and thus form an infinite chain. Although there is a different surrounding around Cu in the dimers they are not displaced significantly different from the basal O_4 planes in CuO_4N (0.201 Å) and CuO_4O (0.198 Å) chromophores, respectively in **1B**, and by 0.197 Å for CuO_4N in **2**. The search through the Cambridge Structural Database [18] revealed that this seems to be the first example where nicotinamide molecule acts as bidentate bridging ligand. This type of arrangement allows an intramolecular hydrogen bond [N(2)–H(22)···O(41), 2.889(4)] between amido nitrogen and carboxylate oxygen. The chain is stabilized in a zigzag distribution of the dimers. This is probably the reason for the reduction of the angle between the planes of the amide group and the pyridine ring from 21° in isolated dimers (**2**) to 11° (**1B**). The network of intermolecular hydrogen bonds in a dimeric compound is distinctly more extensive as in the polymeric one because of a larger number of amino hydrogen atoms on each dimer and an intramolecular hydrogen bond present in **1B**.

The dimeric species (**2**) free of included water molecules shows the geometry of the C_i-symmetric complex to be unchanged from that reported previously for **3** [11]; all of the bond lengths and angles are the same within statistical significance. The principal difference between both complexes is in the intermolecular hydrogen bonding scheme. In the unsolvated complex, the terminal amide groups of lattice translated molecules, are linked via pairs of N–H···O hydrogen bonds to form extended sinuous ribbons. The amide hydrogen atom not involved in the formation of these ribbons serves to cross-link adjacent ribbons via an N–H···O hydrogen bond to one of the acetate oxygen atoms [O(8)] thereby forming hydrogen bonded sheets as illustrated in Fig. 3. This pattern of cross-linking is also present in the solvated structure [11] and the only perturbation imposed by the water molecules is their insertion as a hydrogen bonded spacer within the amide–amide linkages [Fig. 3(a)]. Additional water molecules make the hydrogen bonding network even more extensive thus forming layers of the dimers in the structure. The pattern of π–π stacking of the pyridine rings remains unaffected (mean interplanar separation 3.56 Å, centroid···centroid distance 3.80 Å).

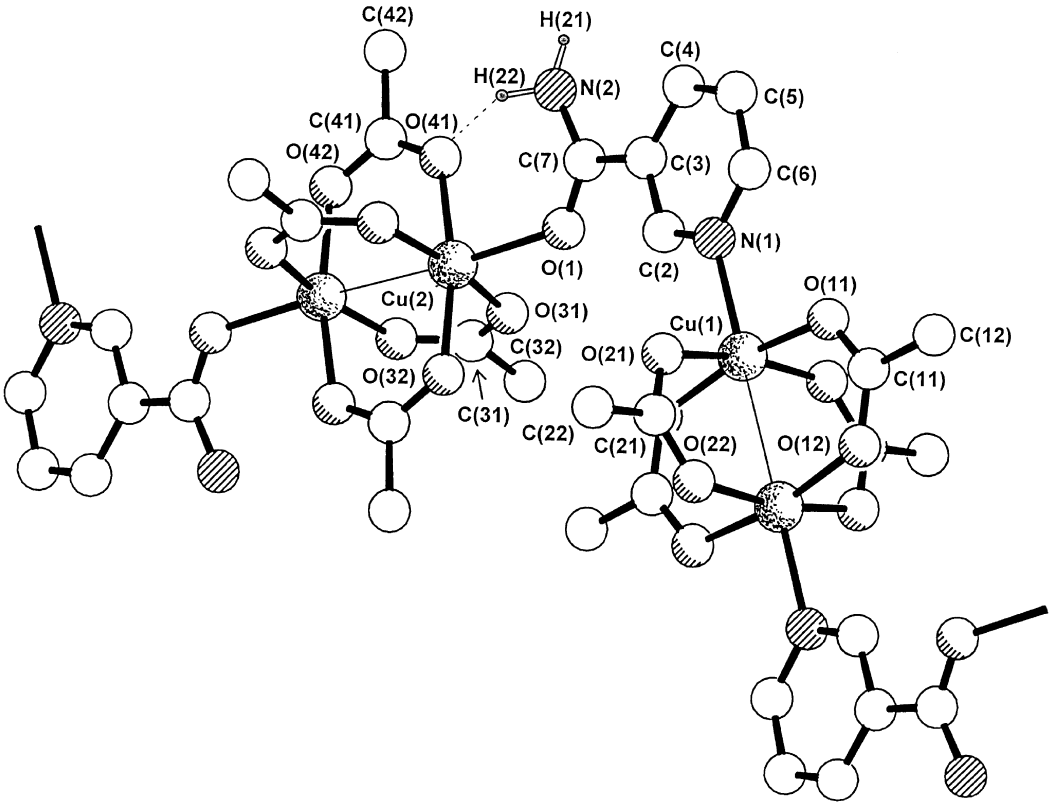

Fig. 1. Representation of the polymeric compound with bidentate bridging nicotinamide molecule and intramolecular hydrogen bond (**1B**). The Cu···Cu separations are 2.628(1) and 2.621(1) Å for both dimers in an asymmetric unit.

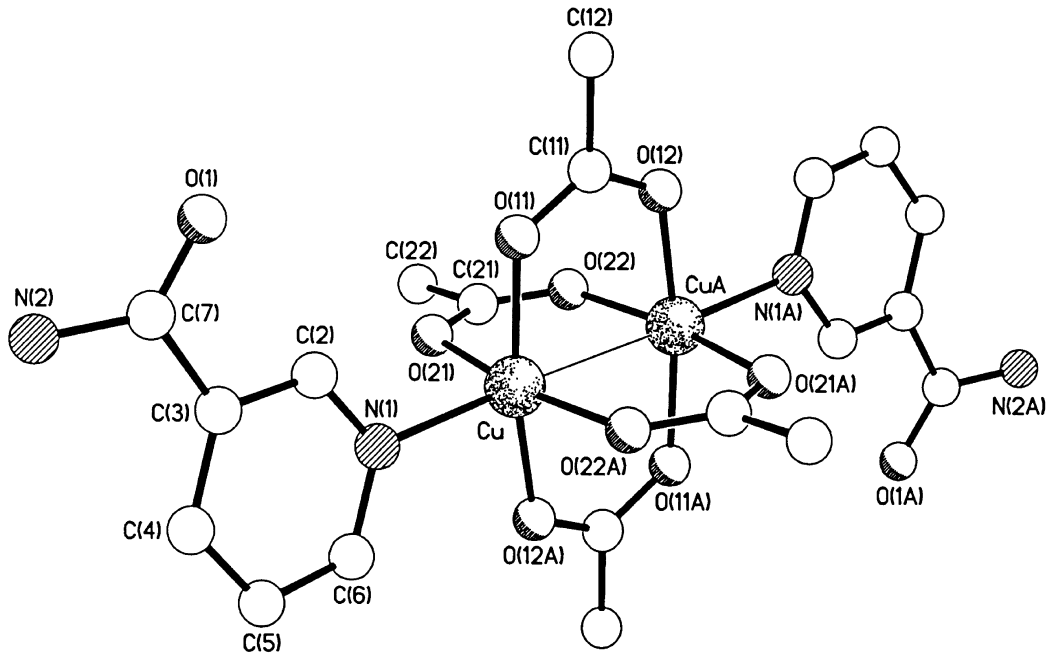

Fig. 2. The molecular structure of isolated dimer in **2**. The Cu···Cu separation is 2.614(1) Å.

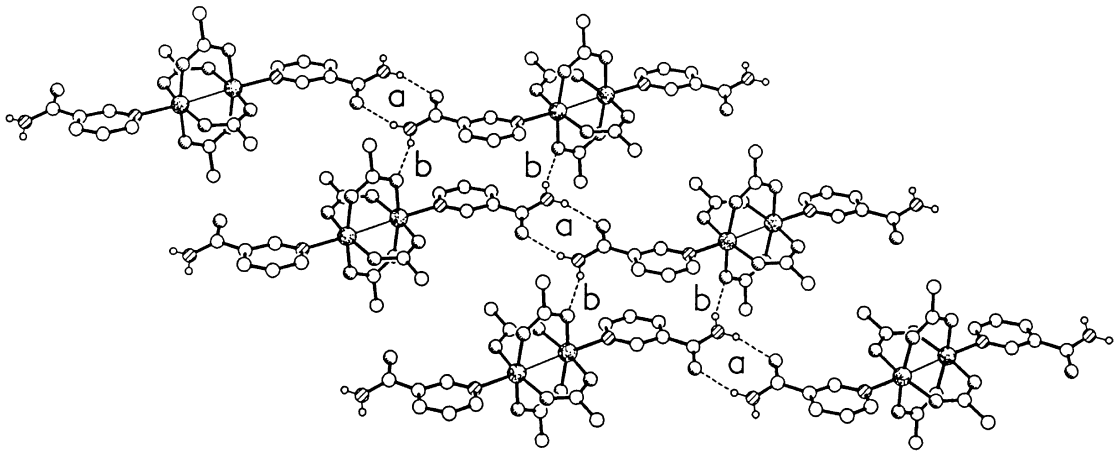

Fig. 3. Part of one hydrogen-bonded sheets of molecules present in the structure of **2** showing the end to end chain formation (a) and the cross-linking interaction (b). The N–H···O hydrogen bondings geometries are: N···O and –H···O distances (Å) and N–H···O angles (°); (a) 2.88, 2.00, 165; (b) 2.95, 2.12, 154 (all of the N–H distances have been normalised to 0.90 Å).

3.2. EPR data

For all four compounds triplet EPR spectra at ambient temperature and at 150 K were observed. Such spectra, characteristic of two interacting Cu(II), already studied in detail, can be described by the spin Hamiltonian, given by the following expression [13, 17, 19]:

$$H=\beta HgS+D[S_z^2-1/3S(S+1)]+E(S_x^2-S_y^2)$$

where D and E are the zero-field splitting parameters, x, y and z are the principal coordinate axes and $S=1$. The other symbols have their usual meaning. Because of the strong antiferromagnetic interaction, the spin Hamiltonian parameter D contains the exchange parameter J, arising from the exchange and dipole–dipole interactions [13]:

$$D=-J/8[1/4(g_{\|}-2)^2-(g_{\perp}-2)^2]-[g_{\|}^2+1/2(g_{\perp}^2)]\beta^2/r^3$$

where r is the distance between two interacting paramagnetic centers. It was shown [20] for dimeric copper(II) carboxylates, that $|2J|$, the singlet–triplet energy gap, is mainly determined by the nature of the RCOOH bridging ligand itself and cannot be unambiguously correlated with other structural parameters such as the type of axial ligand L_{ax} or the distance Cu–L_{ax}. In X-band, the value of D is greater than the microwave energy and only four signals are observed. In addition, when the value of E is very small or even equal to zero, the spectrum will consist only of three lines. This is the case for all compounds at room temperature and for **1A** and **1B** at 150 K (Fig. 4). EPR spectroscopic parameters of room temperature measurements are presented in the Table 4. The values of all four parameters, $g_{\|}$, $g_{\perp}$, D and $|2J|$, lie within the expected ranges [21]. In contrast to **1A** and **1B**, significant changes of EPR spectra line shapes were observed for **2** and **3**, when lowering the temperature to 150 K. The lines corresponding to $H_{\perp}$ split, showing that E is not equal to zero due to deviation from axial symmetry. The same was reported for **3** [17]. The low temperature spectrum of **3** is very complex, exhibiting many additional lines (Fig. 5). Resonance lines of H_{z1} and H_{z2} are split because of the coupling of the electron with two equivalent copper nuclei in dimeric unit. However, no attempt was made to explain other additional lines in this complex EPR spectrum. Hyper-fine splitting parameters for mononuclear impurities were much better resolved at 150 K (compound **1A**: $g_{\|}=2.42$, $g_{\perp}=2.06$, $A_{\|}=17.5$ mT; **1B**: $g_{\|}=2.53$, $g_{\perp}=2.07$; **2**: $g_{\perp}=2.07$; the missing data could not be determined).

The X-ray analysis revealed that three synthesized

Table 4
Room temperature EPR parameters for the studied copper(II) acetates

Compound	H_{z1} (mT)	$H_{\perp}$ (mT)	H_{z2} (mT)	$g_{\|}$	$g_{\perp}$	D (cm^{-1})	$\|2J\|$ (cm^{-1})
1A	24.0	473	604	2.366	2.09	0.346	*
1B	14.0	470	600	2.341	2.09	0.335	324
2	13.5	473	595	2.361	2.12	0.335	396
3	29.0	475	613	2.350	2.09	0.351	324

*The value was not determined because the Cu–Cu distance is not known.

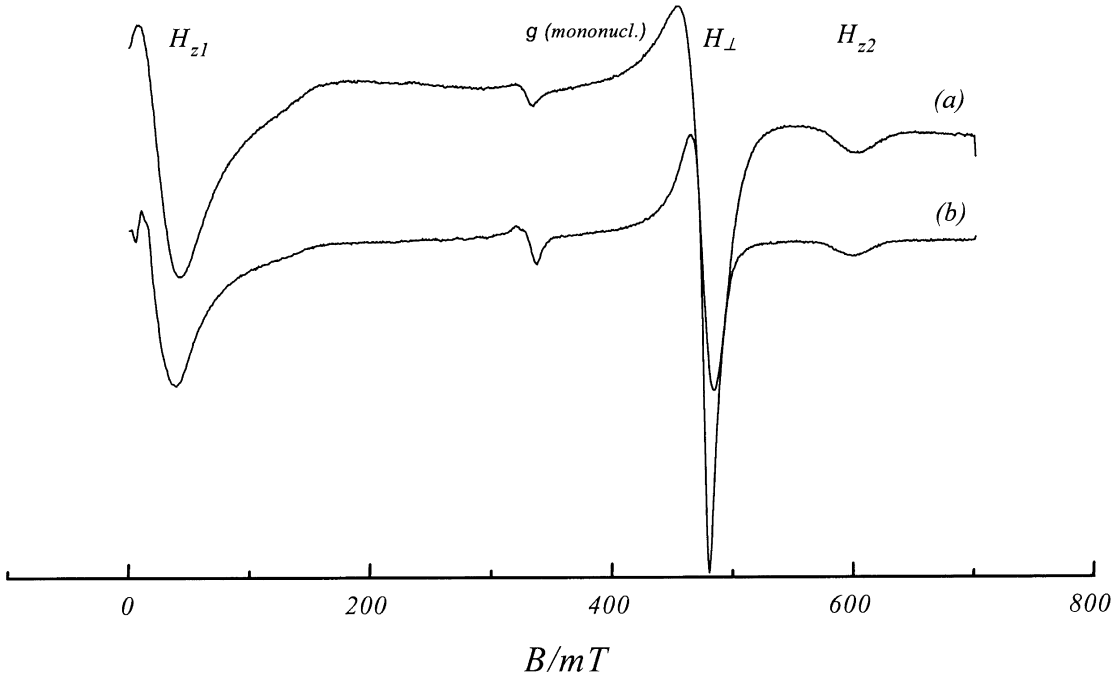

Fig. 4. EPR spectra of **1A**, recorded at (a) room temperature and at (b) 150 K.

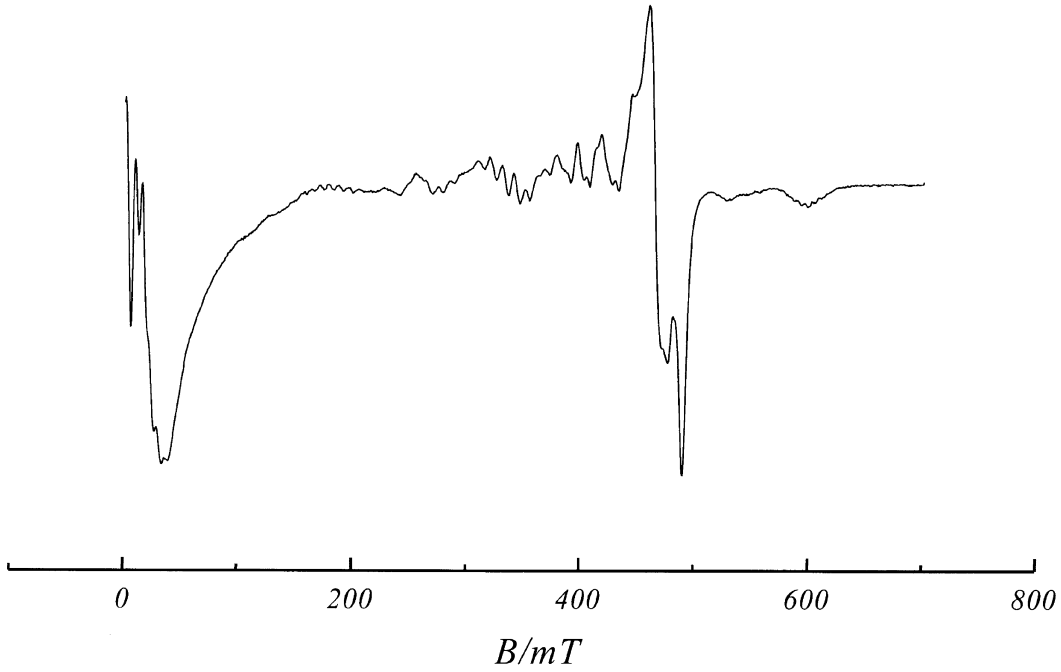

Fig. 5. EPR spectrum of **3**, recorded at 150 K.

compounds are composed of dimeric tetraacetates that are either bonded together (**1B**) or isolated (**2**, **3**). From the results of the other applied characterization methods described above we may also suggest the dimeric nature for the fourth (**1A**) compound [3, 22, 23]. According to the low temperature EPR spectra and the stoichiometry, the structure of **1A** is probably more related to **1B**.

3.3. Fungicidal activity

All synthesized compounds, dissolved in water or DMSO completely stop mycelial growth at a concentration of 5.0×10^{-3} mol l^{-1} although compounds **2** and **3** (dissolved in water) partially recrystallize in cooled culture medium. Less concentrated solutions (up to

1.0×10^{-3} mol l^{-1}) show weaker fungicidal activity. Despite new type of bonding mode of the constituents in the compound **1B**, we didn't observe significant changes in fungicidal activity according to the classical tetracarboxylate type in the complexes **2** and **3**.

Acknowledgements

The work was supported by The Ministry of Science and Technology, Republic of Slovenia, through grant J1-7313-103. EPR spectra were recorded in the EPR center at "Jožef Stefan" Institute in Ljubljana and discussed with Dr M. Šentjurc. We appreciate her useful and fruitful comments. For technical assistance we thank also M. Gruden.

References

[1] Mehrotra, RC, Bohra R. Metal Carboxylates. London: Academic Press, 1983.
[2] Melnik M. Coord Chem Rev 1982;42:259.
[3] Kato M, Muto Y. Coord Chem Rev 1988;92:45.
[4] Sundberg MR, Uggla R, Melrilk M. Polyhedron 1996;15:1157.
[5] Sorensen, JRJ. In: Sigel H, editor. Metal ions in biological systems, Vol. 14, New York: Marcel Dekker, 1982;77.
[6] Richardson BA. Wood Preservation, 2nd edn. E&FN Spon, an imprint of Chapman and Hall, London, 1993.
[7] Pohleven F, Šentjurc M, Petič M, Dagarin F. Holzforschung 1994;48:371.
[8] Pohleven F, Petrič M. International Research Group of Wood Preservation. Document No.: IRG/WP 96-30109. 1996.
[9] Gabe EJ, LePage Y, Charland JP, Lee FL, White PS. J Appl Cryst 1989;22:384.
[10] Civadze AYu, Cincadze GV, Haritonov YaYu, Gverdciteli LV. Zh Neorg Khim 1978;23(2):447.
[11] Cincadze GV, Kiguradze PA, Šiulin AN, Mamedov NS. Zh Strukt Khim 1984;25(6):82.
[12] Harish SP, Sobhanadri J. Inorg Chim Acta 1985;108:147.
[13] Smith TD, Pilbrow JR. Coord Chem Rev 1974;13:173.
[14] Sheldrick GM. SHELXL93. Program for the Refinement of the Crystal Structures. University of Göttingen, Germany, 1993.
[15] SHELXTL PC version 5.03. Siemens Analytical X-ray Instruments, Madison, WI, 1994.
[16] Bergant T, Petrič M, Pohleven F, Reberšek J, Šegedin P. Acta Chim Slov 1994;41:393.
[17] Valko M, Bilton RF, Morris H, Melnik M. J Coord Chem 1993;29:257.
[18] Allen FH, Kennard O. Chem Des Autom News 1993;8:31.
[19] Sapina F, Burgos M, Escriva E, Folgado JV, Beltran D, Gomez-Romero P. Inorg Chim Acta 1994;216:185 (and refs. therein).
[20] Battaglia LP, Bonamartini Corradi A, Menabue, L. J Chem. Soc. Dalton Trans 1986;1653.
[21] Catterick J, Thornton P. Adv Inorg Chem Radiochem 1977;20:291.
[22] Lever ABP. Inorganic Electronic Spectroscopy, 2nd edn. Amsterdam: Elsevier, 1984.
[23] Deacon GB, Philips RJ. Coord Chem Rev 1980;33:227.